



1
2 **Fast and Slow Responses of Atlantic Meridional Overturning**
3 **Circulation to Antarctic Meltwater Forcing**

4
5 Yechul Shin¹, Xin Geng², Ji-Hoon Oh¹, Kyung-Min Noh³, Emilia Kyung Jin⁴,
6 and Jong-Seong Kug^{1*}

7
8 ¹School of Earth and Environmental Sciences, Seoul National University, Seoul, South Korea

9 ²CIC-FEMD/ILCEC, Key Laboratory of Meteorological Disaster of Ministry of Education
10 (KLME), Nanjing University of Information Science and Technology, Nanjing, China.

11 ³National Oceanic and Atmospheric Administration, Office of Oceanic and Atmospheric
12 Research, Geophysical Fluid Dynamics Laboratory, Princeton, USA

13 ⁴Institute Korea Polar Research Institute (KOPRI), Incheon, Republic of Korea

14
15 *Corresponding author: Jong-Seong Kug (jskug1@gmail.com)

16 **Key Points:**

- 17 • The response of the AMOC to perennial meltwater-induced cooling is investigated by
18 GFDL CM2.1 experiments
- 19 • Before the cooling spreads out the Atlantic, tropical atmospheric teleconnection could
20 weaken the Greenland ocean convection
- 21 • The fast and slow responses imply the importance of the atmospheric teleconnection
22 to regulate polar climate
- 23

24 **Abstract**

25 Antarctic meltwater discharge has been largely emphasized for its potential role in
26 climate change mitigation, not only by reducing global warming, but also by stabilizing the
27 Atlantic Meridional Overturning Circulation (AMOC). Despite the tremendous impact of the
28 AMOC on the climate system, its temporal evolution in response to the meltwater remains
29 poorly understood. Here, we investigate the meltwater impacts on the AMOC based on the
30 GFDL CM2.1 experiments and discover its fast weakening and slow strengthening to the
31 Antarctic meltwater discharge. Cold ocean surface caused by meltwater spread throughout
32 the globe and eventually strengthened the AMOC. However, in the early stages, the tropical
33 temperature response could stimulate the Rossby wave teleconnection, modulating
34 atmospheric circulation in the North Atlantic, and weakening convection and even the
35 AMOC. This counterintuitive evolution implies a potential destabilizing effect of Antarctic
36 meltwater, underscoring the importance of the atmospheric dynamics in the interaction
37 between the two poles.

38

39 **Plain Language Summary**

40 The climate system is made up of interactions between different subsystems, so that
41 regional climate changes can have global effects. The freshwater discharge from Antarctica
42 would increase in the future and result in regional cooling. Atmospheric and oceanic
43 dynamics extend this local effect to the globe, reducing global surface temperature and
44 strengthening the large-scale ocean circulation in the Atlantic. These mitigating effects
45 naturally put the spotlight on Antarctic meltwater. Our study however suggests that the
46 mitigation effect depends on the time scale. Although the global mean temperature is always
47 reduced, the ocean circulation in the Atlantic surprisingly slows down as an early response to
48 Antarctic meltwater; fast atmospheric teleconnection enables it. This non-monotonic
49 evolution emphasizes the importance of the atmospheric teleconnection between the two
50 poles, which should be carefully considered to understand the polar climate.

51

52

53 1. Introduction

54 The growing discharge of freshwater into the Southern Ocean (SO) from the
55 Antarctic ice melt is one of the undeniable observations and the anticipated consequences of
56 global warming. Recent satellite data indicate that Antarctic mass loss has increased sharply
57 over the past 40 years (e.g., Rignot et al., 2019; Shepherd et al., 2018), and this trend is
58 projected to continue in the next century (DeConto & Pollard, 2016; Hansen et al., 2016).
59 The mass redistribution has been largely highlighted because it will contribute not only to the
60 global sea level rise (Hanna et al., 2020) but also to a substantial response of the regional
61 climate system associated with distinct structures of the SO (e.g., Bintanja et al., 2013). The
62 ocean circulation surrounding Antarctica is characterized by a cold surface layer and a warm
63 circumpolar deep water (CDW). As meltwater flows into the salty ocean, the low density
64 further reduces ocean mixing, thereby inhibiting CDW upwelling (Fogwill et al., 2015), even
65 though the horizontal gradient of ocean temperature and salinity under ice shelf could induce
66 small-scale mixing and horizontal intrusion (Na et al., 2023). The CDW isolation modulates
67 the biogeochemical properties of the SO (Bronse laer et al., 2020; Oh et al., 2022) and leads to
68 increased sea-ice extent and decreased SO surface temperature (Park & Latif, 2019; Pauling
69 et al., 2016).

70 Even local changes in extratropical regions can have noticeable effects in other
71 regions: the tropics (e.g., Kang et al., 2020; Shin et al., 2021) and even the opposite
72 extratropics (e.g., Cabré et al., 2017; England et al., 2020a; Shin & Kang, 2021). The
73 meltwater-induced cooling is a representative example of such a global teleconnection,
74 causing a northward shift of the Intertropical Convergence Zone (ITCZ)—a narrow band of
75 rainfall near the equator—and global-wide cooling (Bakker & Prange, 2018; Bronse laer et
76 al., 2018). This cooling pattern is accompanied by local cooling minima in East Asia and the
77 Subpolar Northern Atlantic (SPNA). The former has been proposed to be explained by the
78 atmospheric Rossby wave teleconnection mechanism (Oh et al., 2020). The latter, the so-
79 called cooling hole, is generally associated with the strengthening of the Atlantic Meridional
80 Overturning Circulation (AMOC) (e.g., Buckley & Marshall, 2016; Keil et al., 2020), which
81 suggests that the freshwater injection into the Southern Ocean eventually leads to a positive
82 AMOC response (Li et al., 2023; Weaver et al., 2003). Particularly, this response may help to
83 delay the AMOC collapse and its associated impacts (Sinet et al., 2023; Wunderling et al.,

84 2021). Therefore, the Antarctic meltwater has been widely emphasized for its potential role in
85 mitigating both gradual and abrupt climate change.

86 While much attention has been paid to the impacts of Antarctic meltwater, less has
87 been paid to its temporal evolution. It may be acceptable to pay less investigation given the
88 slow time scale of ocean adjustment. However, the interplay between the atmospheric and the
89 oceanic pathways could be of great importance in formulating climate responses on different
90 time scales. For example, the Arctic sea-ice loss could lead to dramatically different impacts
91 between longer multidecadal and shorter decadal time scales (Liu & Fedorov, 2019). They
92 showed that considerable time is required for the slow AMOC response to overcome the
93 global atmospheric teleconnection induced by sea-ice loss, ultimately resulting in split
94 climate patterns with respect to the time scale. Given that Antarctic meltwater input could
95 lead to AMOC responses and also to atmospheric Rossby wave teleconnection, it is natural
96 and reasonable to investigate the potential role of the Antarctic meltwater forcing in the
97 AMOC and regional climate variations across various time scales.

98 The primary purpose of this study is accordingly to investigate the impact of
99 Antarctic meltwater input on the AMOC and its temporal evolution. We conduct a series of
100 experiments to identify the impact of meltwater input. Our findings reveal that an interplay
101 between the atmospheric and oceanic pathways can result in a non-monotonic response of the
102 AMOC to the Antarctic meltwater input: early weakening and late strengthening. This non-
103 monotonic response emphasizes the connection between the two polar regions in regulating
104 climate response to external forcing.

105

106 **2. Model and experiment**

107 In this study, we employ a fully coupled model, CM2.1, developed at the
108 Geophysical Fluid Dynamics Laboratory (Delworth et al., 2006). The atmosphere and land
109 models have a nominal 2° horizontal resolution, and the ocean and ice models have a nominal
110 1° horizontal resolution. We start with a 2000-year control simulation (CTL) at an
111 atmospheric carbon dioxide concentration of 353 ppm, representing the 1990 level. The first
112 1,000 years are discarded to avoid long-term drift and the last 1,000 years are used as initial
113 conditions for forced ensemble experiments. We conducted two forced experiments for 12

114 ensemble members, each integrated from every 50 years of the last 1000 years of the control
115 experiment. One is the MW_off experiment, which is solely forced by atmospheric carbon
116 dioxide (CO₂) concentration that increases at a rate of 1% yr⁻¹ for 70 years and then remains
117 at doubled CO₂ concentration (706 ppm). The other is the MW_on experiment, which is not
118 only forced by the same radiative forcing, but also by an idealized Antarctic meltwater input.
119 The meltwater forcing is introduced at the surface, assuming that it results from ice-
120 sheet/shelf melting. The meltwater forcing is a time-invariant 0.2 Sv freshwater discharge,
121 equivalent to a sea level rise of 1.6 cm per year. This aligns with the expected amount around
122 2050 under the Representative Concentration Pathway 8.5 scenarios (DeConto & Pollard,
123 2016). Considering contributions from large icebergs, the anticipated timeframe could be
124 earlier than 2050 (e.g., England et al., 2020b). The meltwater distribution is injected
125 proportional to the climatological runoff of Antarctica into the Southern Ocean. Thus, the
126 majority of the meltwater is concentrated around West Antarctica, as indicated by recent
127 observations (Rignot et al., 2019; Shepherd et al., 2018). The difference between the two
128 experiments indicates the impact of Antarctic meltwater: $\delta = MW_{on} - MW_{off}$.

129 The statistical significance of meltwater impacts, δ , is measured by a bootstrap
130 analysis that calculates the 95% confidence level between the 25th and 975th values among
131 randomly generated 1,000 bootstrap samples. Note that this set of experiments shares a
132 general design with previous studies investigating Antarctic meltwater impacts (Oh et al.,
133 2022; Park & Latif, 2019).

134

135 **3. Result**

136 The impact of Antarctic meltwater on global climate is shown in Figure 1. Doubling
137 CO₂ warms the global mean surface temperature by 1.6 K without meltwater input (red in
138 Figure 1a). As previous studies suggested, the Antarctic meltwater reduces surface warming
139 (blue in Figure 1a). The global cooling effect peaks at year 31, reaching -0.41 K, and then
140 gradually weakens (Figure 1b). Note that this gradual weakening of the cooling effect is
141 commonly reported in studies using time-invariant meltwater input (e.g., Park and Latif 2019;
142 Oh et al. 2020), regarded as the compensation of subsurface warming with limited heat
143 reservoir of the deep ocean (Martin et al., 2013; L. Zhang & Delworth, 2016). Nevertheless,
144 the meltwater input always reduces global mean surface warming.

145 Meltwater-induced cooling is strongest in the SO following geographic adjacency,
146 especially near West Antarctica (Figure 1e). This cooling extends to the entire Southern
147 Hemisphere and tropics, even in the Arctic (e.g., Bronselaer et al., 2018). In addition, the
148 tropical precipitation shows a distinct pattern: a zonal-mean northward shift and a weakening
149 of walker circulation (green-brown contour in Figure 1e). The former has been relatively
150 well-established since the early 2000s, first noticed by paleoclimate proxies and modeling
151 experiments (e.g., Chiang & Bitz, 2005; Peterson et al., 2000). Theoretical studies suggest
152 that the zonal-mean precipitation is shifted to the north which reduces the meltwater-induced
153 interhemispheric energy asymmetry (e.g., Kang et al., 2018a). The latter is more related to the
154 Walker cell response to the forcing. The employed model produces weakened convection at
155 the warm pool to the Antarctic meltwater, which is consistently shown in other models
156 imposing the Antarctic meltwater forcing (see Figure 2 in Bronselaer et al., 2018; Figure 2 in
157 Oh et al., 2020).

158 In climate models, the AMOC is generally expected to weaken under global warming
159 (e.g., Levang & Schmitt, 2020; Reintges et al., 2017), and the Antarctic meltwater is expected
160 to counteract the weakening. Consistently, in our experiments, the meltwater input tends to
161 strengthen the AMOC, measuring the maximum meridional stream function at 45°N, after the
162 cooling peaks. However, although the meltwater ultimately mitigates the impacts of global
163 warming on the AMOC (Figures 1c-d), the meltwater discharge unexpectedly weakens the
164 AMOC beforehand (Figure 1d). Internal variability may obscure the weakening in some
165 members. Nevertheless, it is evident that the meltwater-forced AMOC response depends
166 significantly on the time scale, which is consistently shown in the SPNA temperature (Figure
167 S1a). Considering that the temperature response generally retains its pattern with respect to
168 the time (Figure S1b), the AMOC response to the meltwater-induced cooling shows not a
169 simple linear but a non-monotonic relationship, which is counterintuitive to the large inertia
170 of the ocean circulation that would be expected to produce a more gradual response to the
171 perennial cooling.

172 To understand this non-monotonic response in detail, we look at the periods before
173 and after the sign reversal of δ AMOC, referred to as weak (year 6-20) and strong (year 31-
174 45) periods (orange and gray shading in Figure 1). We first note that, although the AMOC
175 responses are opposite, the zonal-mean ocean circulation response in the SO and tropics is
176 somewhat similar (Figures 1f-g). In the southern extratropics, the freshwater input reduces

177 the formation of Antarctic Bottom Water, while the cold surface intensifies a meridional
178 temperature gradient and westerly winds, accompanied by enhanced Deacon cell (Park &
179 Latif, 2019). In the tropics, the northward ITCZ shift indicates a weakening of the northern
180 Hadley cell, and vice versa. Since the atmospheric and oceanic circulation are mechanically
181 coupled through surface wind stress, subtropical cell responses mirror the changes occurring
182 on the Hadley cell (Held, 2001), compensating meltwater-induced interhemispheric
183 asymmetry (e.g., Green & Marshall, 2017; Kang et al., 2018b; Schneider, 2017). Only in the
184 northern extratropics the oceanic circulation is dependent on the time scale. During the strong
185 period, the AMOC generally strengthens (Figure 1g), which is consistent with previous
186 studies reporting the long-term response of the AMOC to meltwater input and/or the surface
187 cooling hole (Bronse laer et al., 2018; Oh et al., 2020; Park & Latif, 2019). However, just a
188 few years after the freshwater forcing, the AMOC experiences a significant weakening. Note
189 that it closely resembles the response of the AMOC to freshwater input from Greenland, the
190 antipode of Antarctica (Figure 1f; Figures 6a-c in Li et al., 2023).

191 Focusing on the weak period, we examine the temporal evolution of upper-ocean
192 density in the Atlantic basin (Figure 2). The density responses are most pronounced above
193 500 m, suggesting that upper-level stratification plays an important role in regulating the
194 AMOC (Figure S2; Zhang et al., 2017). The Hovmöller diagram shows that the Atlantic
195 upper-ocean density suddenly decreases at the northern high-latitudes at the beginning of the
196 weak period, which corresponds to the weakening of the AMOC (Figures 2a and S2a). The
197 density reduction is solely pronounced in the deep convection region of the AMOC, the
198 Labrador Sea (Figure 2b), where even small perturbations can induce large AMOC responses
199 (e.g., Stocker & Wright, 1991). Salinity plays a dominant role in driving the density decrease.
200 Although cold temperature has the potential to increase the density (Figure 2g-h), it cannot
201 overcome surface freshening (Figure 2d-e). Note that these regions have been proposed to be
202 diluted by freshwater fluxes from Greenland (Gillard et al., 2016), which partially explains
203 the aforementioned similarity with the results of the Greenland freshwater hosing experiment
204 (Li et al., 2023).

205 The local stratification is eventually terminated by Atlantic-wide cooling. Although
206 local freshening continues to weaken the AMOC (Figures 2d-f), thermally-driven density
207 anomalies emerge from low-latitudes and propagate northward through the upper ocean,
208 gradually overcoming the stratification at the deep convection region (Figures 2a-c and S2).

209 Temperature anomalies evolve along the Atlantic water pathway (Figure S3), implying the
210 importance of climatological upper-ocean circulation in regulating SPNA convection (e.g.,
211 Piecuch et al., 2017). Within a few decades, the whole North Atlantic upper ocean, as well as
212 the SPNA, is eventually de-stratified by thermal contraction. It is followed by a strengthening
213 of the AMOC and a cessation of the weak periods. This time scale is comparable to previous
214 results, showing that it takes a few decades for tropical salinity to spread throughout the
215 North Atlantic (see Figure S12 in Hu & Fedorov, 2019), and we note that the near-surface (0-
216 5 m) density evolution is almost consistent with that in the upper ocean (Figure S4). Taken
217 together, the density profiles clearly indicate that some rapid response to the Antarctic
218 meltwater input abruptly dilutes the deep convection regions near Greenland, leading to an
219 unrecognized weakening of the AMOC.

220 Atmospheric processes are intuitively the most likely candidate for abrupt salinity
221 reduction, not only because of their fast time scale but also because of the importance of
222 large-scale atmospheric circulation in regulating salinity (e.g., Durack et al., 2012). Thermal
223 forcing imposed in the SO could influence tropical climate through the lower troposphere,
224 leading to changes in the tropical hydrological cycle within a few years (Kim et al., 2022). As
225 the tropical convection is modulated, the resulting Gill-type response could rapidly perturb
226 the extratropical climate via the wave train propagating poleward and eastward (Hoskins &
227 Karoly, 1981). Hence, we examine the precipitation and 300hPa stream function response at
228 the onset of the weak period (Figure 3a). Suppressed convection is detected in the western
229 Pacific warm pool region, which excites upper-level cyclonic flow and the wave energy
230 continues to propagate northeastward across North America. The associated wave activity
231 flux (WAF) suggests that the wave propagation eventually gives rise to the anticyclonic
232 circulation over Greenland, which projects onto a negative NAO pattern. The teleconnection
233 is quite similar to that shown in previous studies which suggest a strong positive correlation
234 between western Pacific convection and NAO response (e.g., Geng et al., 2023; Huntingford
235 et al., 2014; Scaife et al., 2017). Note that the wave train is consistently shown in the boreal
236 winter (DJF), when both the Rossby wave teleconnection and the SPNA deep convection are
237 dominant (Figure S5). The NAO is known to modulate the AMOC intensity through the
238 surface buoyancy response in the deep convection regions, a relationship corroborated by
239 many climate models, including the employed model (e.g., Delworth & Zeng, 2016; Kim et
240 al., 2023; Medhaug et al., 2012). In alignment with this, the presence of an anticyclone over

241 Greenland corresponds to a weakening of the surface westerly winds over the SPNA,
242 resulting in a significant reduction of regional evaporation (Figure 3b). While regional
243 precipitation shows a slight decrease with the anticyclone (not shown), the downward water
244 flux at the surface—precipitation minus evaporation (P-E)—shows a significant increase mainly
245 due to the evaporation reduction. This increase explains the salinity drop at the onset of weak
246 periods, inducing feeble convection at the Labrador Sea (Figure 2a,e).

247 We further analyzed the 1000-year control experiment to consolidate the tropical-
248 induced salinity decrease over the SPNA. To establish a link between the high-latitude
249 circulation response to tropical convection, we initially remove the time-mean value from the
250 1000-year precipitation data, thereby representing interannual precipitation variability. Linear
251 regression analysis is then performed for each year, regressing the interannual variability
252 pattern against the meltwater-induced precipitation pattern (depicted by the dashed box in
253 Figure 3a). As a result, the regression coefficient quantifies the spatial similarity of the
254 precipitation variability to the target precipitation pattern, the meltwater-induced response.
255 Therefore, we repeat linear regressions that the pattern regression coefficient is regressed
256 with respect to the interannual variability of the 300 hPa stream function, surface wind speed,
257 and evaporation at each grid, which allows us to extract the atmospheric variability when the
258 tropical convection resembles the meltwater-induced response (Figures 3c-d).

259 The extracted precipitation pattern does not fit perfectly with that forced by the
260 Antarctic meltwater (contour in Figure 3c), as the former mostly reflects zonal redistribution
261 of diabatic heating, while the latter represents a combination of meridional shift and zonal
262 redistribution. However, the western Pacific diabatic cooling induces a similar wave train that
263 propagates northeastward to the SPNA, leading to anticyclonic circulation over Greenland
264 (Figure 3c). In line with the change at the onset of the weak period, we also observe a
265 subsequent decrease in both surface wind speed and evaporation (Figure 3d), although these
266 changes are smaller than the forced response associated with the weaker anticyclone. The
267 difference in background climates, one representing the present climate and the other the
268 early stage of global warming, may contribute to the different amplitude in the circulation
269 responses over Greenland. Nevertheless, strong correlations between forced and regression
270 patterns, particularly 0.82 for evaporation and 0.71 for surface wind speed (dashed box in
271 Figure 3b), highlight a spatial similarity over the Labrador and Irminger Seas. The spatial

272 resemblance underscores the crucial role of atmospheric teleconnection in regulating the
273 climate of the North Atlantic.

274 **4. Summary and Discussion**

275 In this study, we investigate the impact of Antarctic meltwater on the AMOC with
276 particular interest in its temporal evolution. Previous studies have shown that Antarctic
277 meltwater induces global cooling, and both the atmosphere and the ocean circulation adjust to
278 it, such as the northward shift of the ITCZ and the strengthening of the Deacon cell
279 (Bronseleer et al., 2018; Park & Latif, 2019). However, our study suggests that while the
280 AMOC strengthening is stably detected after 30 years of simulation, it is unexpectedly
281 weakened during the initial period by the Antarctic meltwater discharge, which makes a non-
282 monotonic AMOC response to global cooling (Figure 4). The non-monotonic response is
283 attributed to the differing timescales of atmospheric and oceanic teleconnections. The SO
284 cooling could affect the tropical climate within a few years through near-surface propagation,
285 resulting in convection redistribution (Kang et al., 2023; Kim et al., 2022). Then, the
286 suppressed convection immediately triggers an upper-level cyclonic flow, which initiates
287 Rossby wave propagation to the extratropics. Before the Atlantic gyre system brings tropical
288 cooling into the SPNA convection region that is followed by the AMOC strengthening, the
289 wave-induced anticyclone over Greenland, which is a polarity of the negative NAO pattern,
290 weakens the surface westerlies, evaporation, and the strength of the AMOC. Therefore, the
291 non-monotonic response of the AMOC, consistently shown as a tug-of-war in the SPNA
292 upper-ocean density, is the result of competing influences between atmospheric
293 teleconnection, which induces rapid and regional freshening, and oceanic propagation, which
294 results in slow but strong thermal stratification.

295 We do not want to overemphasize our findings via the single model: the non-
296 monotonicity examined would be model-dependent. For example, the AMOC is known as
297 notorious spread among current climate models (e.g., Gong et al., 2022). Thus, even if the
298 atmospheric teleconnection rapidly adjusts the AMOC, the magnitude of the adjustment
299 would be highly variable across models (e.g., Kim et al., 2023). In addition, although the
300 tropical response is similar to that shown in the studies imposing the Antarctic meltwater
301 (Bronseleer et al., 2018; Oh et al., 2020), some models project a similar weakened convection
302 in response to the Antarctic sea-ice loss, which accompanies with surface warming (e.g.,

303 Ayres et al., 2022; England et al., 2020c). Hence, the sensitivity of the tropical response to
304 either forcing structures or model configurations would have a potential to modulate the non-
305 monotonicity. All of these factors underscore the importance of the model intercomparison to
306 the realistic Antarctic meltwater impacts. As the next generation of Coupled Model
307 Intercomparison Project (CMIP7) is planned to include an interactive meltwater (e.g., Swart
308 et al., 2023), further studies are warranted that carefully examine the meltwater-induced
309 tropical response and consequent AMOC response.

310 Despite the plausible amount of meltwater under global warming (DeConto &
311 Pollard, 2016), employing an abrupt and time-invariant injection may exaggerate the
312 temporal evolution of the meltwater impacts. In the context of global warming, a gradual
313 increase in meltwater discharge consistently induces relative cooling in the Southern Ocean,
314 contributing to AMOC weakening by the atmosphere and strengthening by the ocean.
315 However, the time scale of each adjustment would not be differentiated, resulting in blurred
316 atmospheric impacts. It's important to note that wind variability substantially influences the
317 Southern Ocean temperature (Roach et al., 2023), and constructive interference with the
318 meltwater flux still holds the potential for non-monotonic AMOC responses. Overall,
319 however, the non-monotonic evolution is less anticipated with gradual meltwater alone.

320 In other words, the non-monotonicity is more likely to occur when sudden and
321 disastrous changes happen, which aligns with the growing concern about various tipping
322 elements (McKay et al., 2022) and their interaction, referred to as tipping cascading
323 (Wunderling et al., 2023). Our current understanding of these cascading impacts is still
324 limited to conceptual and idealized models. For example, conceptual models that consider the
325 oceanic transport alone propose the abrupt meltwater discharge from the West Antarctic Ice
326 Sheet (WAIS) as a potential stabilizing factor for the AMOC (Sinet et al., 2023). However,
327 our findings point out a new dimension that the WAIS could also provoke AMOC
328 destabilization through the atmospheric pole-to-pole teleconnection. Note that there are
329 alternative pathways that could link SPNA and tropical climate such as Indo-Pacific Ocean
330 (e.g., Hu & Fedorov, 2020; Orihuela-Pinto et al., 2023). Considering the intricate nature of
331 climate systems, further studies are warranted to carefully investigate the meltwater impacts
332 on both gradual and abrupt climate change by employing a more realistic configuration. The
333 primary purpose of this study, however, is to highlight the potential of non-monotonic AMOC
334 response by the interplay between atmosphere and ocean pathways.

335 **Acknowledgments**

336 This research was supported by Korea Institute of Marine Science & Technology Promotion
337 (KIMST) funded by the Ministry of Oceans and Fisheries (RS-2023-00256677; PM23020)
338 and by the National Research Foundation of Korea (NRF) grant funded by the Korean
339 government (NRF-2022R1A3B1077622)

340

341 **Data Availability Statement**

342 The processed data of the simulations used for this study is available in Shin (2023).

343

344

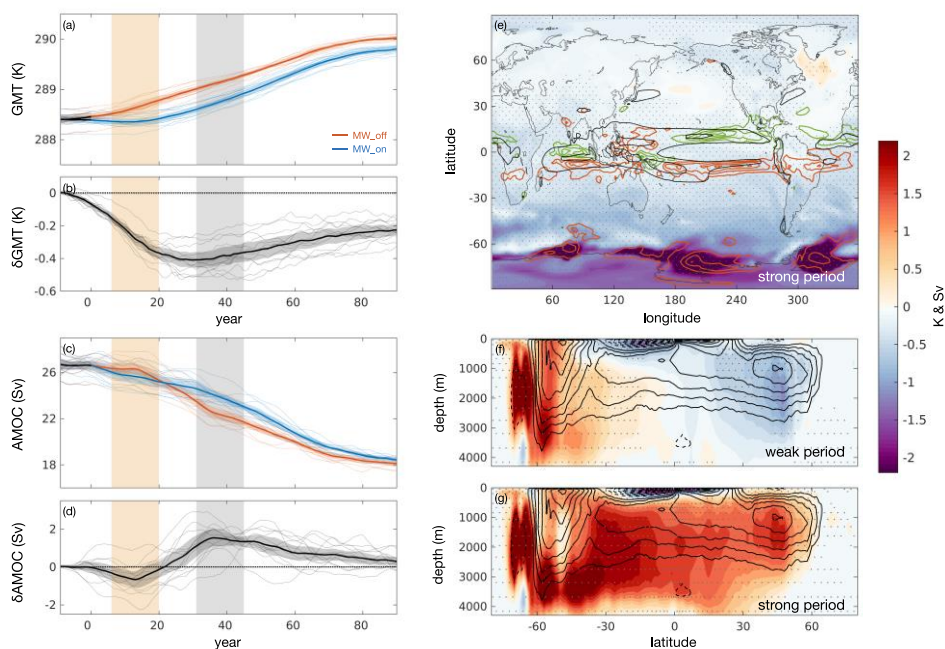
345 **Reference**

- 346 Armstrong McKay, D. I., Staal, A., Abrams, J. F., Winkelmann, R., Sakschewski, B., Loriani, S., et al.
 347 (2022). Exceeding 1.5°C global warming could trigger multiple climate tipping points.
 348 *Science*, 377(6611), eabn7950. <https://doi.org/10.1126/science.abn7950>
- 349 Ayres, H. C., Screen, J. A., Blockley, E. W., & Bracegirdle, T. J. (2022). The Coupled Atmosphere–
 350 Ocean Response to Antarctic Sea Ice Loss. *Journal of Climate*, 35(14), 4665–4685.
 351 <https://doi.org/10.1175/JCLI-D-21-0918.1>
- 352 Bakker, P., & Prange, M. (2018). Response of the Intertropical Convergence Zone to Antarctic Ice
 353 Sheet Melt. *Geophysical Research Letters*, 45(16), 8673–8680.
 354 <https://doi.org/10.1029/2018GL078659>
- 355 Bintanja, R., van Oldenborgh, G. J., Drijfhout, S. S., Wouters, B., & Katsman, C. A. (2013). Important
 356 role for ocean warming and increased ice-shelf melt in Antarctic sea-ice expansion. *Nature*
 357 *Geoscience*, 6(5), 376–379. <https://doi.org/10.1038/ngeo1767>
- 358 Bronselaer, B., Winton, M., Griffies, S. M., Hurlin, W. J., Rodgers, K. B., Sergienko, O. V., et al.
 359 (2018). Change in future climate due to Antarctic meltwater. *Nature*, 564(7734), 53–58.
 360 <https://doi.org/10.1038/s41586-018-0712-z>
- 361 Bronselaer, B., Russell, J. L., Winton, M., Williams, N. L., Key, R. M., Dunne, J. P., et al. (2020).
 362 Importance of wind and meltwater for observed chemical and physical changes in the
 363 Southern Ocean. *Nature Geoscience*, 13(1), 35–42. [https://doi.org/10.1038/s41561-019-0502-](https://doi.org/10.1038/s41561-019-0502-8)
 364 8
- 365 Buckley, M. W., & Marshall, J. (2016). Observations, inferences, and mechanisms of the Atlantic
 366 Meridional Overturning Circulation: A review. *Reviews of Geophysics*, 54(1), 5–63.
 367 <https://doi.org/10.1002/2015RG000493>
- 368 Cabré, A., Marinov, I., & Gnanadesikan, A. (2017). Global Atmospheric Teleconnections and
 369 Multidecadal Climate Oscillations Driven by Southern Ocean Convection. *Journal of*
 370 *Climate*, 30(20), 8107–8126. <https://doi.org/10.1175/JCLI-D-16-0741.1>
- 371 Chiang, J. C. H., & Bitz, C. M. (2005). Influence of high latitude ice cover on the marine Intertropical
 372 Convergence Zone. *Climate Dynamics*, 25(5), 477–496. [https://doi.org/10.1007/s00382-005-](https://doi.org/10.1007/s00382-005-0040-5)
 373 0040-5
- 374 DeConto, R. M., & Pollard, D. (2016). Contribution of Antarctica to past and future sea-level rise.
 375 *Nature*, 531(7596), 591–597. <https://doi.org/10.1038/nature17145>
- 376 Delworth, T. L., & Zeng, F. (2016). The Impact of the North Atlantic Oscillation on Climate through
 377 Its Influence on the Atlantic Meridional Overturning Circulation. *Journal of Climate*, 29(3),
 378 941–962. <https://doi.org/10.1175/JCLI-D-15-0396.1>
- 379 Delworth, T. L., Broccoli, A. J., Rosati, A., Stouffer, R. J., Balaji, V., Beesley, J. A., et al. (2006).
 380 GFDL’s CM2 Global Coupled Climate Models. Part I: Formulation and Simulation
 381 Characteristics. *Journal of Climate*, 19(5), 643–674. <https://doi.org/10.1175/JCLI3629.1>
- 382 Durack, P. J., Wijffels, S. E., & Matear, R. J. (2012). Ocean Salinities Reveal Strong Global Water
 383 Cycle Intensification During 1950 to 2000. *Science*, 336(6080), 455–458.
 384 <https://doi.org/10.1126/science.1212222>
- 385 England, Mark R., Polvani, L. M., & Sun, L. (2020a). Robust Arctic warming caused by projected
 386 Antarctic sea ice loss. *Environmental Research Letters*, 15(10), 104005.
 387 <https://doi.org/10.1088/1748-9326/abaada>
- 388 England, Mark R., Wagner, T. J. W., & Eisenman, I. (2020b). Modeling the breakup of tabular
 389 icebergs. *Science Advances*, 6(51), eabd1273. <https://doi.org/10.1126/sciadv.abd1273>
- 390 England, Mark R., Polvani, L. M., Sun, L., & Deser, C. (2020c). Tropical climate responses to
 391 projected Arctic and Antarctic sea-ice loss. *Nature Geoscience*, 13(4), 275–281.
 392 <https://doi.org/10.1038/s41561-020-0546-9>
- 393 Fogwill, C. J., Phipps, S. J., Turney, C. S. M., & Golledge, N. R. (2015). Sensitivity of the Southern
 394 Ocean to enhanced regional Antarctic ice sheet meltwater input. *Earth’s Future*, 3(10), 317–
 395 329. <https://doi.org/10.1002/2015EF000306>
- 396 Geng, X., Zhao, J., & Kug, J.-S. (2023). ENSO-driven abrupt phase shift in North Atlantic oscillation

- 397 in early January. *Npj Climate and Atmospheric Science*, 6(1), 1–8.
 398 <https://doi.org/10.1038/s41612-023-00414-2>
- 399 Gillard, L. C., Hu, X., Myers, P. G., & Bamber, J. L. (2016). Meltwater pathways from marine
 400 terminating glaciers of the Greenland ice sheet. *Geophysical Research Letters*, 43(20),
 401 10,873–10,882. <https://doi.org/10.1002/2016GL070969>
- 402 Gong, X., Liu, H., Wang, F., & Heuzé, C. (2022). Of Atlantic Meridional Overturning Circulation in
 403 the CMIP6 Project. *Deep Sea Research Part II: Topical Studies in Oceanography*, 206,
 404 105193. <https://doi.org/10.1016/j.dsr2.2022.105193>
- 405 Green, B., & Marshall, J. (2017). Coupling of Trade Winds with Ocean Circulation Damps ITCZ
 406 Shifts. *Journal of Climate*, 30(12), 4395–4411. <https://doi.org/10.1175/JCLI-D-16-0818.1>
- 407 Hanna, E., Pattyn, F., Navarro, F., Favier, V., Goelzer, H., van den Broeke, M. R., et al. (2020). Mass
 408 balance of the ice sheets and glaciers – Progress since AR5 and challenges. *Earth-Science
 409 Reviews*, 201, 102976. <https://doi.org/10.1016/j.earscirev.2019.102976>
- 410 Hansen, J., Sato, M., Hearty, P., Ruedy, R., Kelley, M., Masson-Delmotte, V., et al. (2016). Ice melt,
 411 sea level rise and superstorms: evidence from paleoclimate data, climate modeling, and
 412 modern observations that 2 °C global warming could be dangerous. *Atmospheric Chemistry
 413 and Physics*, 16(6), 3761–3812. <https://doi.org/10.5194/acp-16-3761-2016>
- 414 Held, I. M. (2001). The Partitioning of the Poleward Energy Transport between the Tropical Ocean
 415 and Atmosphere. *Journal of the Atmospheric Sciences*, 58(8), 943–948.
 416 [https://doi.org/10.1175/1520-0469\(2001\)058<0943:TPOTPE>2.0.CO;2](https://doi.org/10.1175/1520-0469(2001)058<0943:TPOTPE>2.0.CO;2)
- 417 Hu, S., & Fedorov, A. V. (2019). Indian Ocean warming can strengthen the Atlantic meridional
 418 overturning circulation. *Nature Climate Change*, 9(10), 747–751.
 419 <https://doi.org/10.1038/s41558-019-0566-x>
- 420 Hu, S., & Fedorov, A. V. (2020). Indian Ocean warming as a driver of the North Atlantic warming
 421 hole. *Nature Communications*, 11(1), 4785. <https://doi.org/10.1038/s41467-020-18522-5>
- 422 Huntingford, C., Marsh, T., Scaife, A. A., Kendon, E. J., Hannaford, J., Kay, A. L., et al. (2014).
 423 Potential influences on the United Kingdom’s floods of winter 2013/14. *Nature Climate
 424 Change*, 4(9), 769–777. <https://doi.org/10.1038/nclimate2314>
- 425 Kang, S. M., Shin, Y., & Xie, S.-P. (2018). Extratropical forcing and tropical rainfall distribution:
 426 energetics framework and ocean Ekman advection. *Npj Climate and Atmospheric Science*,
 427 1(1), 1–10. <https://doi.org/10.1038/s41612-017-0004-6>
- 428 Kang, S. M., Shin, Y., & Codron, F. (2018). The partitioning of poleward energy transport response
 429 between the atmosphere and Ekman flux to prescribed surface forcing in a simplified GCM.
 430 *Geoscience Letters*, 5(1), 22. <https://doi.org/10.1186/s40562-018-0124-9>
- 431 Kang, S. M., Xie, S.-P., Shin, Y., Kim, H., Hwang, Y.-T., Stuecker, M. F., et al. (2020). Walker
 432 circulation response to extratropical radiative forcing. *Science Advances*, 6(47), eabd3021.
 433 <https://doi.org/10.1126/sciadv.abd3021>
- 434 Kang, S. M., Shin, Y., Kim, H., Xie, S.-P., & Hu, S. (2023). Disentangling the mechanisms of
 435 equatorial Pacific climate change. *Science Advances*, 9(19), eadf5059.
 436 <https://doi.org/10.1126/sciadv.adf5059>
- 437 Keil, P., Mauritsen, T., Jungclaus, J., Hedemann, C., Olonscheck, D., & Ghosh, R. (2020). Multiple
 438 drivers of the North Atlantic warming hole. *Nature Climate Change*, 10(7), 667–671.
 439 <https://doi.org/10.1038/s41558-020-0819-8>
- 440 Kim, H., Kang, S. M., Kay, J. E., & Xie, S.-P. (2022). Subtropical clouds key to Southern Ocean
 441 teleconnections to the tropical Pacific. *Proceedings of the National Academy of Sciences*,
 442 119(34), e2200514119. <https://doi.org/10.1073/pnas.2200514119>
- 443 Kim, H.-J., An, S.-I., Park, J.-H., Sung, M.-K., Kim, D., Choi, Y., & Kim, J.-S. (2023). North Atlantic
 444 Oscillation impact on the Atlantic Meridional Overturning Circulation shaped by the mean
 445 state. *Npj Climate and Atmospheric Science*, 6(1), 1–13. <https://doi.org/10.1038/s41612-023-00354-x>
- 447 Levang, S. J., & Schmitt, R. W. (2020). What Causes the AMOC to Weaken in CMIP5? *Journal of
 448 Climate*, 33(4), 1535–1545. <https://doi.org/10.1175/JCLI-D-19-0547.1>
- 449 Li, Q., Marshall, J., Rye, C. D., Romanou, A., Rind, D., & Kelley, M. (2023). Global Climate Impacts

- 450 of Greenland and Antarctic Meltwater: A Comparative Study. *Journal of Climate*, 1(aop), 1–
 451 40. <https://doi.org/10.1175/JCLI-D-22-0433.1>
- 452 Liu, W., & Fedorov, A. V. (2019). Global Impacts of Arctic Sea Ice Loss Mediated by the Atlantic
 453 Meridional Overturning Circulation. *Geophysical Research Letters*, 46(2), 944–952.
 454 <https://doi.org/10.1029/2018GL080602>
- 455 Martin, T., Park, W., & Latif, M. (2013). Multi-centennial variability controlled by Southern Ocean
 456 convection in the Kiel Climate Model. *Climate Dynamics*, 40(7), 2005–2022.
 457 <https://doi.org/10.1007/s00382-012-1586-7>
- 458 Medhaug, I., Langehaug, H. R., Eldevik, T., Furevik, T., & Bentsen, M. (2012). Mechanisms for
 459 decadal scale variability in a simulated Atlantic meridional overturning circulation. *Climate*
 460 *Dynamics*, 39(1), 77–93. <https://doi.org/10.1007/s00382-011-1124-z>
- 461 Na, J. S., Davis, P. E. D., Kim, B., Jin, E. K., & Lee, W. S. (2023). Ice Shelf Water Structure Beneath
 462 the Larsen C Ice Shelf in Antarctica. *Geophysical Research Letters*, 50(19), e2023GL104088.
 463 <https://doi.org/10.1029/2023GL104088>
- 464 Oh, J.-H., Park, W., Lim, H.-G., Noh, K. M., Jin, E. K., & Kug, J.-S. (2020). Impact of Antarctic
 465 Meltwater Forcing on East Asian Climate Under Greenhouse Warming. *Geophysical*
 466 *Research Letters*, 47(21), e2020GL089951. <https://doi.org/10.1029/2020GL089951>
- 467 Oh, J.-H., Noh, K. M., Lim, H.-G., Jin, E. K., Jun, S.-Y., & Kug, J.-S. (2022). Antarctic meltwater-
 468 induced dynamical changes in phytoplankton in the Southern Ocean. *Environmental Research*
 469 *Letters*, 17(2), 024022. <https://doi.org/10.1088/1748-9326/ac444e>
- 470 Orihuela-Pinto, B., Santoso, A., England, M. H., & Taschetto, A. S. (2023). Coupled Feedbacks From
 471 the Tropical Pacific to the Atlantic Meridional Overturning Circulation. *Geophysical*
 472 *Research Letters*, 50(20), e2023GL103250. <https://doi.org/10.1029/2023GL103250>
- 473 Park, W., & Latif, M. (2019). Ensemble global warming simulations with idealized Antarctic
 474 meltwater input. *Climate Dynamics*, 52(5), 3223–3239. <https://doi.org/10.1007/s00382-018-4319-8>
- 475 Pauling, A. G., Bitz, C. M., Smith, I. J., & Langhorne, P. J. (2016). The Response of the Southern
 476 Ocean and Antarctic Sea Ice to Freshwater from Ice Shelves in an Earth System Model.
 477 *Journal of Climate*, 29(5), 1655–1672. <https://doi.org/10.1175/JCLI-D-15-0501.1>
- 478 Peterson, L. C., Haug, G. H., Hughen, K. A., & Röhl, U. (2000). Rapid Changes in the Hydrologic
 479 Cycle of the Tropical Atlantic During the Last Glacial. *Science*, 290(5498), 1947–1951.
 480 <https://doi.org/10.1126/science.290.5498.1947>
- 481 Piecuch, C. G., Ponte, R. M., Little, C. M., Buckley, M. W., & Fukumori, I. (2017). Mechanisms
 482 underlying recent decadal changes in subpolar North Atlantic Ocean heat content. *Journal of*
 483 *Geophysical Research: Oceans*, 122(9), 7181–7197. <https://doi.org/10.1002/2017JC012845>
- 484 Reintges, A., Martin, T., Latif, M., & Keenlyside, N. S. (2017). Uncertainty in twenty-first century
 485 projections of the Atlantic Meridional Overturning Circulation in CMIP3 and CMIP5 models.
 486 *Climate Dynamics*, 49(5), 1495–1511. <https://doi.org/10.1007/s00382-016-3180-x>
- 487 Rignot, E., Mouginot, J., Scheuchl, B., van den Broeke, M., van Wessem, M. J., & Morlighem, M.
 488 (2019). Four decades of Antarctic Ice Sheet mass balance from 1979–2017. *Proceedings of*
 489 *the National Academy of Sciences*, 116(4), 1095–1103.
 490 <https://doi.org/10.1073/pnas.1812883116>
- 491 Roach, L. A., Mankoff, K. D., Romanou, A., Blanchard-Wrigglesworth, E., Haine, T. W. N., &
 492 Schmidt, Gavin. A. (2023). Winds and Meltwater Together Lead to Southern Ocean Surface
 493 Cooling and Sea Ice Expansion. *Geophysical Research Letters*, 50(24), e2023GL105948.
 494 <https://doi.org/10.1029/2023GL105948>
- 495 Scaife, A. A., Comer, R. E., Dunstone, N. J., Knight, J. R., Smith, D. M., MacLachlan, C., et al.
 496 (2017). Tropical rainfall, Rossby waves and regional winter climate predictions. *Quarterly*
 497 *Journal of the Royal Meteorological Society*, 143(702), 1–11. <https://doi.org/10.1002/qj.2910>
- 498 Schneider, T. (2017). Feedback of Atmosphere-Ocean Coupling on Shifts of the Intertropical
 499 Convergence Zone. *Geophysical Research Letters*, 44(22), 11,644–11,653.
 500 <https://doi.org/10.1002/2017GL075817>
- 501 Shepherd, A., Fricker, H. A., & Farrell, S. L. (2018). Trends and connections across the Antarctic
 502

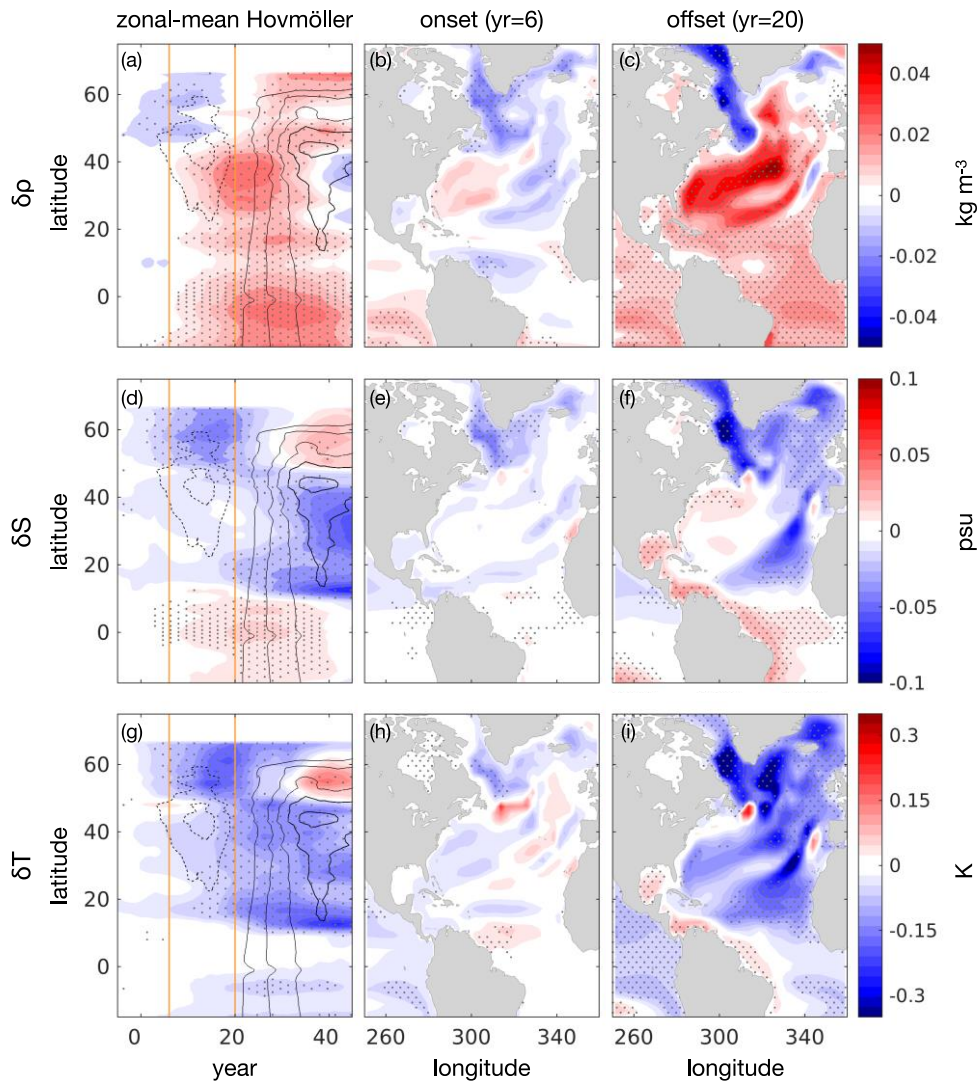
- 503 cryosphere. *Nature*, 558(7709), 223–232. <https://doi.org/10.1038/s41586-018-0171-6>
- 504 Shin, Y., & Kang, S. M. (2021). How Does the High-Latitude Thermal Forcing in One Hemisphere
505 Affect the Other Hemisphere? *Geophysical Research Letters*, 48(24), e2021GL095870.
506 <https://doi.org/10.1029/2021GL095870>
- 507 Shin, Y., Kang, S. M., Takahashi, K., Stuecker, M. F., Hwang, Y.-T., & Kim, D. (2021). Evolution of
508 the Tropical Response to Periodic Extratropical Thermal Forcing. *Journal of Climate*, 1(aop),
509 1–53. <https://doi.org/10.1175/JCLI-D-20-0493.1>
- 510 Shin, Y. (2023). Ensemble experiment to investigate Antarctic meltwater input under global warming
511 by GFDL CM2.1 [Dataset]. Zenodo . <https://doi.org/10.5281/zenodo.10056446>
- 512 Sinet, S., von der Heydt, A. S., & Dijkstra, H. A. (2023). AMOC Stabilization Under the Interaction
513 With Tipping Polar Ice Sheets. *Geophysical Research Letters*, 50(2), e2022GL100305.
514 <https://doi.org/10.1029/2022GL100305>
- 515 Stocker, T. F., & Wright, D. G. (1991). Rapid transitions of the ocean’s deep circulation induced by
516 changes in surface water fluxes. *Nature*, 351(6329), 729–732.
517 <https://doi.org/10.1038/351729a0>
- 518 Swart, N. C., Martin, T., Beadling, R., Chen, J.-J., Danek, C., England, M. H., et al. (2023). The
519 Southern Ocean Freshwater Input from Antarctica (SOFIA) Initiative: scientific objectives
520 and experimental design. *Geoscientific Model Development*, 16(24), 7289–7309.
521 <https://doi.org/10.5194/gmd-16-7289-2023>
- 522 Weaver, A. J., Saenko, O. A., Clark, P. U., & Mitrovica, J. X. (2003). Meltwater Pulse 1A from
523 Antarctica as a Trigger of the Bølling-Allerød Warm Interval. *Science*, 299(5613), 1709–
524 1713. <https://doi.org/10.1126/science.1081002>
- 525 Wunderling, N., Donges, J. F., Kurths, J., & Winkelmann, R. (2021). Interacting tipping elements
526 increase risk of climate domino effects under global warming. *Earth System Dynamics*, 12(2),
527 601–619. <https://doi.org/10.5194/esd-12-601-2021>
- 528 Wunderling, N., von der Heydt, A., Aksenov, Y., Barker, S., Bastiaansen, R., Brovkin, V., et al. (2023).
529 Climate tipping point interactions and cascades: A review. *EGUsphere*, 1–45.
530 <https://doi.org/10.5194/egusphere-2023-1576>
- 531 Zhang, L., & Delworth, T. L. (2016). Impact of the Antarctic bottom water formation on the Weddell
532 Gyre and its northward propagation characteristics in GFDL CM2.1 model. *Journal of*
533 *Geophysical Research: Oceans*, 121(8), 5825–5846. <https://doi.org/10.1002/2016JC011790>
- 534 Zhang, X., Knorr, G., Lohmann, G., & Barker, S. (2017). Abrupt North Atlantic circulation changes in
535 response to gradual CO2 forcing in a glacial climate state. *Nature Geoscience*, 10(7), 518–
536 523. <https://doi.org/10.1038/ngeo2974>
- 537

538 **Figure list**

539

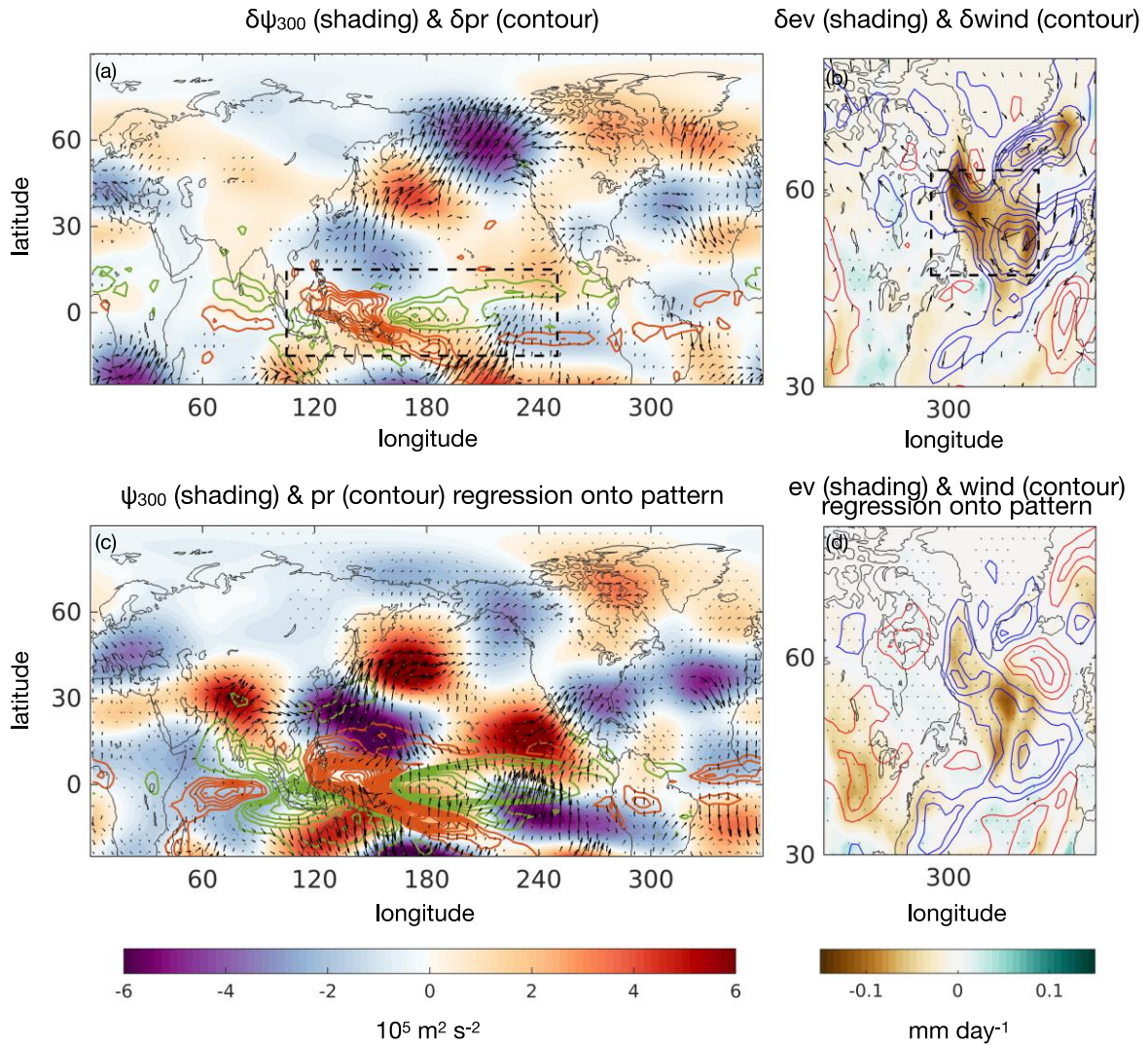
540 **Figure 1.** Time series of (a) global mean surface temperature. Red is the ensemble with CO₂
 541 doubling only (MW_off), while blue is the ensemble with additional Antarctic meltwater
 542 discharge (MW_on). (b) Meltwater-induced response in global mean surface temperature
 543 (i.e., blue-red). (c,d) Same time series as (a,b), but for the AMOC index, measuring the
 544 maximum meridional stream function at 45°N. Every time series is smoothed by 21-yr
 545 running average. Each ensemble members are shown as a thin line, with its mean as a thick
 546 line. Shading indicates the statistical range at the 95% confidence level. Gray vertical shading
 547 indicates a strong period (year 31-45) regarding δ AMOC, while orange shading indicates a
 548 weak period (year 6-20). (e) Meltwater-induced surface temperature (shading) and
 549 precipitation (interval = 0.13 mm day⁻¹; positive in green and negative in brown) anomalies at
 550 the strong period. Black solid contour is climatological precipitation (interval = 5 mm day⁻¹).
 551 (f) Response of the MOC to the meltwater (shading) at the weak period and (g) at the strong
 552 period. Climatological MOC is shown in solid-dashed contour (interval = 3 Sv; positive in
 553 solid and negative in dashed). Red shading and solid contour indicate clockwise circulation
 554 and vice versa. Dotted area indicates statistical significance at the 95% confidence level.

555



556

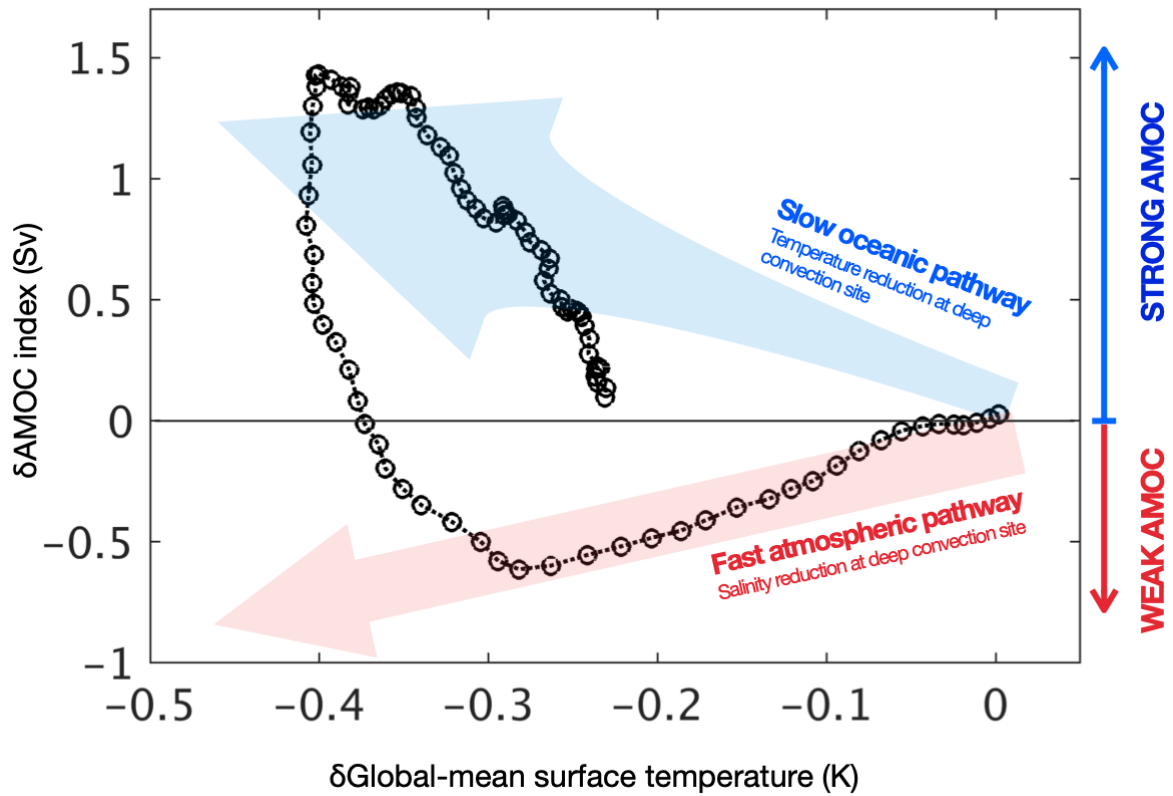
557 **Figure 2.** (left) Atlantic zonal-mean Hovmöller diagram of upper-level (0-500m) (a) density,
 558 (g) salinity, and (g) temperature. The meridional stream function at 1000 m is shown as a
 559 solid-dashed contour (interval = 0.3 Sv; positive in solid and negative in dashed). The onset
 560 and offset of the weak period are shown as orange lines. All variables are 21-year running
 561 averaged. (middle) Anomalous map for corresponding variable at onset and (right) offset.
 562 Dotted area indicates statistical significance at the 95% confidence level.



563

564 **Figure 3.** (a) Annual-mean stream function at 300 hPa (shading), precipitation (interval =
 565 0.12 mm day^{-1} ; positive in green and negative in brown), and wave activity flux (quiver)
 566 anomalies, and (b) evaporation (shading), surface wind speed (interval = 0.015 m s^{-1} ; positive
 567 in red and negative in blue), and 10 m wind (quiver) anomalies to the Antarctic meltwater
 568 input at the onset of weak period (year 6 to 12). (c,d) Same maps as (a,b) but for the
 569 regression coefficient of each variable on the anomalous precipitation pattern. Dotted regions
 570 are statistically significant at the 95% confidence level. The dashed box in (a) indicates the
 571 anomalous precipitation pattern for regression analysis, and that in (b) indicates the Labrador
 572 and Irminger Seas.

573

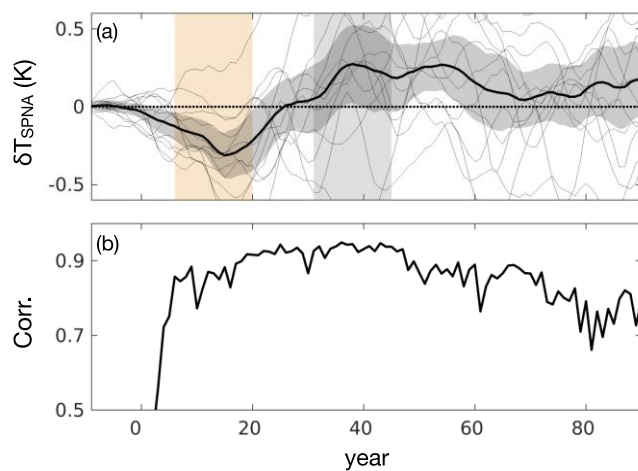


574

575 **Figure 4.** Meltwater-induced AMOC anomalies with respect to the global-mean surface
 576 cooling. Each circle indicates 21-year running-mean value. Although the global-mean
 577 temperature decreases by the meltwater hosing, the AMOC response is muted for the first few
 578 years corresponding to the time lag between Southern Ocean cooling and tropical response.
 579 Then, the AMOC response is not following the intuitive strengthening, but weakening which
 580 is driven by fast atmospheric pathway. As time goes by, slow but strong ocean pathway
 581 reaches the deep convection region, the AMOC exhibits abrupt transition under relatively
 582 consistent global-mean cooling.

583

584

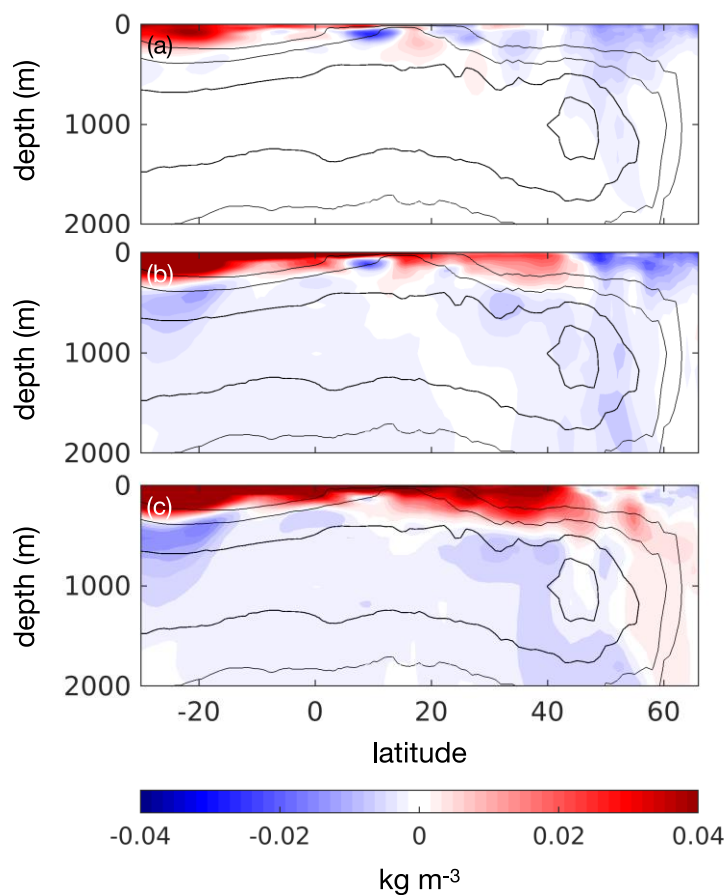


585

586 **Figure S1.** (a) Same time series as Figure 1b but for SPNA surface temperature ($50^{\circ}\text{N}\sim 60^{\circ}\text{N}$,
587 $300^{\circ}\text{E}\sim 320^{\circ}\text{E}$). (b) Time series of pattern correlation coefficient between δT_S at each year and that of
588 strong period, shown in Fig. 1e.

589

590

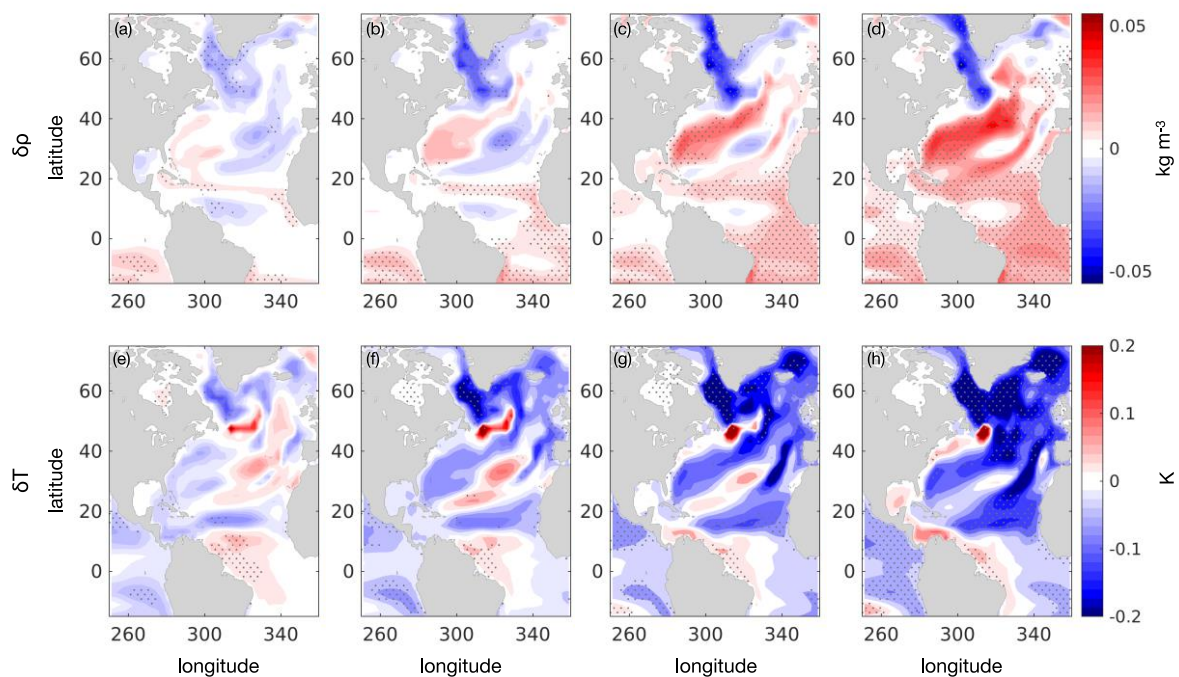


591

592 **Figure S2.** (a) Atlantic depth-latitude profile of the anomalous density response to the Antarctic
 593 meltwater at the onset, (b) middle, (c) offset of the weak period. Climatological mean meridional
 594 stream function is shown in solid contour (interval = 4 Sv).

595

596



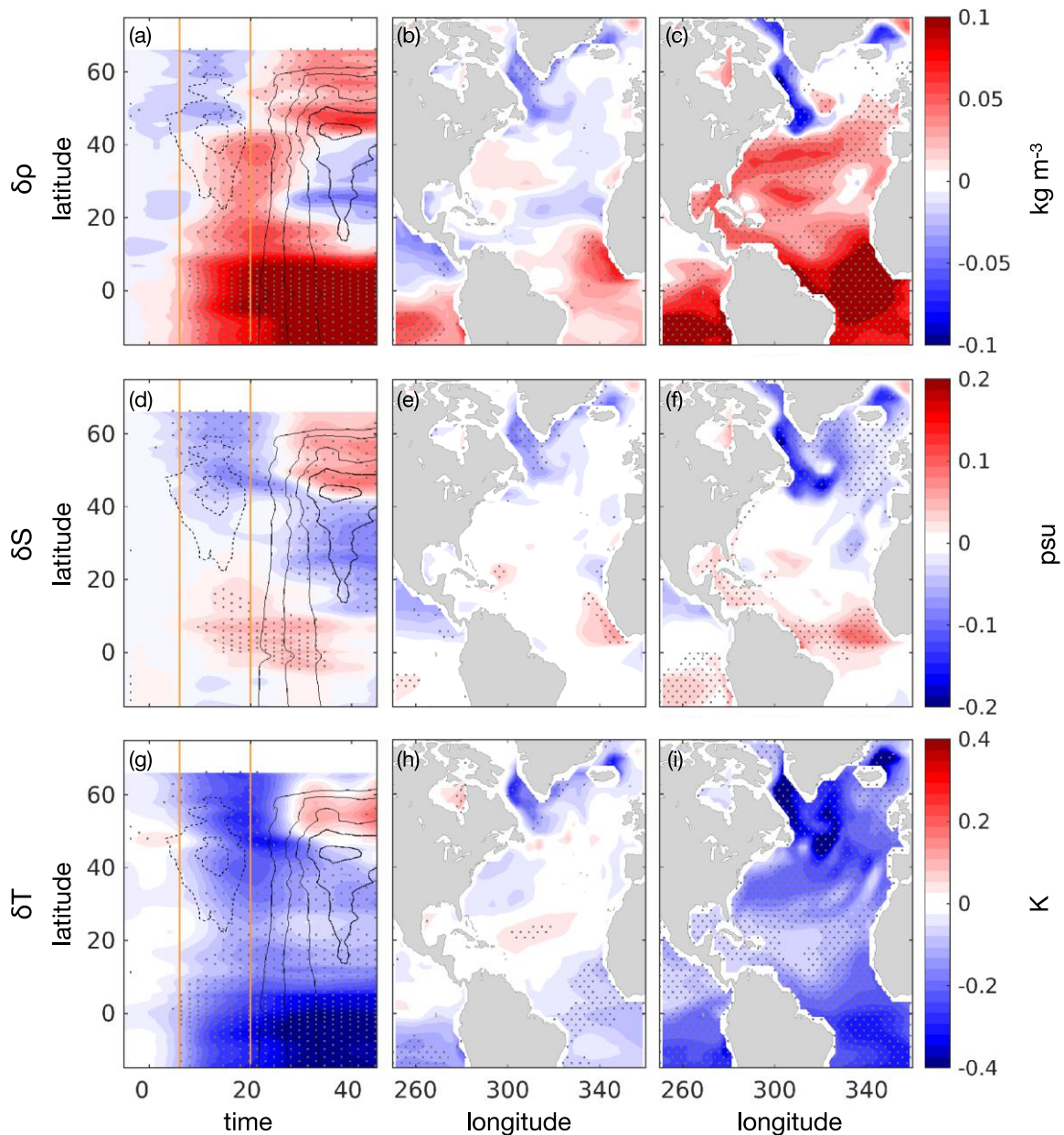
597

598 **Figure S3.** Anomalous map for upper-level (0-500m) density and temperature (a,e) of the onset of the
 599 weak period and (b-d,f-h) every 4 year from thereafter.

600

601

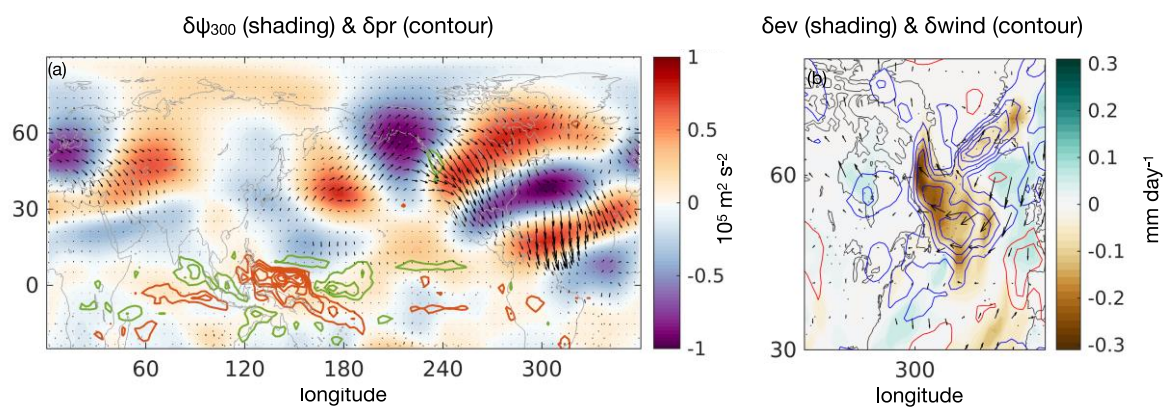
602



603

604 **Figure S4.** Same as Figure 2 but for surface layer.

605



606

607 **Figure S5.** Same as Figure 3a and b but for the boreal winter (DJF).

608